Study of Molecular Orientation by Vibrational Spectroscopy: From Polymers to Silk

*Christian Pellerin, Marie-Eve Rousseau, Mathieu Côté, Michel Pézolet**

CERSIM, Département de chimie, Université Laval, Pavillon Alexandre-Vachon, Québec (Québec) Canada G1K 7P4
E-mail: michel.pezolet@chm.ulaval.ca

Summary: Infrared and Raman spectroscopies are very efficient techniques to characterize molecular orientation in macromolecular systems. In the present paper, two examples of the application of vibrational spectroscopy to the study of molecular orientation in synthetic and natural macromolecules will be presented. In the first example, the dynamics of orientation and relaxation of stretched films of bimodal blends of polystyrene (PS) and deuterated polystyrene (dPS) has been studied *in situ* by polarization modulation infrared linear dichroism while, in the second one, polarized Raman microspectroscopy has been used to determined quantitatively the orientation of β-sheet domains in single filaments of *Bombyx mori* silk.

Keywords: infrared; orientation; polymer blends; Raman; silk

Introduction

Molecular orientation is often introduced in natural and synthetic macromolecules by the mechanical deformation that occurs during their processing. Since molecular orientation strongly affects the physical properties of macromolecular systems, it is important to understand the mechanisms that govern their orientation and relaxation of orientation. To that end, several techniques have been used such as birefringence, X-ray diffraction, NMR spectroscopy, sonic modulus, fluorescence polarization and vibrational spectroscopy.[1] Infrared and Raman spectroscopies are very efficient techniques to characterize molecular orientation since they can provide information about the degree of orientation of different chemical groups or phases in multicomponent systems such as polymer blends, semicrystalline polymers, and copolymers.

Infrared linear dichroism (IRLD) has been widely used to study polymer deformation, but its use is limited to relatively slow processes. To improve the sensitivity of this technique and to allow following accurately the dynamics of orientation and relaxation, FTIR spectroscopy has been coupled with the polarization modulation (PM) technique.[2,3] With PM-IRLD, the dichroic difference spectrum is recorded directly, thus minimizing instrumental and sample fluctuations during the measurement. Polarized Raman spectroscopy using a confocal microscope is also a powerful technique to characterize the orientation of macromolecules. The main advantage of this technique is that the laser beam can be focused down to about 1 μm in diameter on the sample,

 DOI: 10.1002/masy.200550207

therefore allowing the recording of high quality spectra of single fibers. In addition, the second and fourth terms, $\langle P_2 \rangle$ and $\langle P_4 \rangle$, respectively, of the Legendre polynomial expansion of the orientation distribution function can be determined from polarized Raman spectra[4] while only $\langle P_2 \rangle$ can be determined by IRLD. From the knowledge of both $\langle P_2 \rangle$ and $\langle P_4 \rangle$, it is possible to make a more accurate estimation of the orientation distribution function and to discriminate between distributions that would be undistinguishable if only $\langle P_2 \rangle$ was known.

In this paper, two examples of the application of vibrational spectroscopy to the study of molecular orientation in macromolecular systems will be presented. In the first example, the dynamics of orientation and relaxation of stretched films of bimodal blends of polystyrene (PS) and deuterated polystyrene (dPS) has been studied *in situ* by PM-IRLD while, in the second one, polarized Raman microspectroscopy has been used to determine quantitatively the orientation of the β-sheet domains in single filaments of *Bombyx mori* silk.

Experimental Section

Materials

Monodisperse atactic polystyrene (Pressure Chemicals) with molecular weights (M_w) of 942 and 200 kg/mol and perdeuterated polystyrene (Polymer Source) with M_w of 218, 64 and 22 kg/mol were used. The equivalent M_w for the hydrogenated short chains is 202, 59 and 20 kg/mol, respectively. For clarity, they will be referred to as dPS 200, 60 and 20 throughout the rest of the text. All polydispersity indices were below 1.06. Films of 50 μm thickness containing 75% w/w of PS and 25% w/w of dPS were cast on glass plates from 3% benzene solutions. Films were air-dried at room temperature for two days and then gradually heated under vacuum up to 120°C for 48 h to remove the last traces of solvent and residual stresses.

The *Bombyx mori* (*B. mori*) cocoon samples were obtained from the Insects Production Unit of the Canadian Forest Service (Sault-Ste-Marie, Ontario, Canada). To eliminate any organic material, the cocoons were emptied, stirred, and heated at 40°C in a sodium peroxide solution (0.01% m/v) for 30 min.[5] The cocoon fibers were then degummed in boiling water containing sodium bicarbonate (0.5% m/v) for 20 min.[6] The resulting material was rinsed thoroughly with deionized water and dried under vacuum. The degummed silk was solubilized in a 9M lithium bromide solution.[7] The salt was then removed by dialyzing the solution against deionized water for 3 days with daily changes of water using cellulose tubing (12 to 14 kDa cut-off). The regenerated films (thicknesses of about 25 μm) were obtained by casting the dialyzed solution onto polyethylene and dried overnight in dry air.

Methods

PS/dPS films of 20 x 6 mm were stretched to a fixed draw ratio of 2, either at Tg + 15 at a constant draw rate of 100 cm/min or at Tg + 8 at a draw rate of 10 cm/min, using a homebuilt mechanical stretcher. At least five samples were deformed under each experimental condition. Dichroic difference spectra with a resolution of 8 cm^{-1} were obtained *in situ* using a Bomem Michelson MB-100 spectrophotometer equipped with an InSb (EG&G Judson) detector using the optical setup and two-channel electronic processing described elsewhere.[2] All the experiments were conducted in three consecutive acquisition steps: a first series of 180 spectra of 4 scans, followed by 90 spectra of 30 scans, and by a final series of 80 spectra of 75 scans. The second term of the orientation distribution function, $\langle P_2 \rangle$, was calculated from the intensity of the dichroic difference ΔA as:

$$\langle P_2 \rangle = \frac{2}{\left(3\langle \cos^2 \alpha \rangle - 1\right)} \frac{\Delta A}{3A_0} \sqrt{\lambda}$$

where λ is the draw ratio, A_0 is the absorbance of the isotropic (undeformed) sample and α is the average angle between the transition moment of the vibration considered and the main chain axis.

The Raman spectra of silk monofilaments, having less than 20 μm in diameter, were obtained using a LabRam 800HR Raman microspectrometer (Jobin Yvon Horiba, Villeneuve d'Asqc, France) with the 514.5 nm line of an argon ion laser (Spectra-Physics, Model 2020, Mountain View, CA). The laser beam was focused with a 100X objective (0.9 NA-Olympus) to a diameter of approximately 1 μm with an intensity of 4.5 mW at the sample. The confocal hole was fixed at 200 μm and the entrance slit of the monochromator at 100 μm. By using a 600 lines/mm holographic grating, a spectral window of approximately 2000 cm^{-1} was collected for each exposure by the one-inch open electrode Peltier-cooled CCD detector (1024 x 256 pixels) (Andor Technologies, Belfast, Northern Ireland). A half-wave plate (Melles Griot, Carlsbad, CA) was used to orient the polarization of the incident laser beam parallel (X) and perpendicular (Y) to the fiber axis without having to move the sample. An analyzer, which consists of Polaroid® sheets, was placed before the monochromator to selectively detect the polarized scattered light parallel (X) and perpendicular (Y) to the fiber axis. The spectra were obtained from 3 x 60 s and 5 x 30 s integration periods for the fibers and the films, respectively.

All spectra were corrected for the polarization dependence of the notch filter and of the grating. Correction for the grating efficiency was achieved from the ratio of two spectra obtained with a white light source by changing the analyzer polarization. The polarization dependence of the notch filter was measured by recording the spectra of an isotropic sample (carbon tetrachloride) for the two polarization directions of the incident laser beam. The refractive index used for *B. mori* silk

was 1.56. All spectral manipulations were performed using GRAMS/AI (version 7.00) from ThermoGalactic. The spectra were 7-points smoothed and corrected for a small fluorescence background.

Results and Discussion

Dynamics of orientation in PS / dPS blends.

In most fundamental studies of molecular orientation in polymers, samples possessing a narrow molecular weight distribution are used so that the results can be analyzed in the framework of existing theories. In contrast, commercial commodity polymers like PS are often produced by radical polymerization and thus present a rather broad molecular weight distribution, with polydispersity indices usually larger than 2. The production of polydisperse polymers reduces the synthesis costs but strongly modifies the viscoelastic properties of the material as compared to monodisperse samples possessing the same M_w studied in the laboratory. A first step for a better understanding of the orientation development and relaxation in polydisperse polymers is the study of model bimodal blends composed of mixture of short and long monodisperse chains of the same homopolymer. Infrared spectroscopy is a tool of choice to study the molecular orientation in such systems because isotopic labeling enables simultaneous characterization of both types of chains. This approach has already been used in a number of studies on block copolymers containing hydrogenated PS in the center and deuterated PS at the ends[8,9] and in blends of short chains of dPS with long chains of PS.[10-13] Tassin et al. have observed that the orientation developed by the short chains increases with their M_w as well as with that of the long chains forming the matrix, suggesting an orientational coupling in the system.[10] Hayes et al. have noted that the orientation of the long chains is not influenced by the length of the short dPS.[11] In contrast, Bokobza et al. have reported that the orientation of the matrix decreases as compared to the pure homopolymer if the short chains are below their critical molecular weight to form entanglements, M_c.[12,13] This result is in agreement with theoretical simulations[14] as well as with measurements on bimodal blends of poly(methyl methacrylate).[15] All these studies were performed using conventional infrared linear dichroism (IRLD), so the relaxation curves were either obtained indirectly by quenching several samples after various relaxation times, or *in situ* but with a limited time resolution. In this work, we have used PM-IRLD to determine directly with a time resolution of 1.6 s the deformation and relaxation curves of both constituents of bimodal PS blends composed of long hydrogenated PS chains and shorter deuterated PS chains.

Figure 1 shows the infrared spectrum of an undeformed sample of a PS 942 / dPS 200 blend in the

C-H and C-D stretching mode regions (2750-3200 and 2150-2350 cm^{-1}, respectively), as well as three dichroic difference spectra recorded immediately at the end of the deformation (0 s), and after 20 and 1500 s of relaxation. The signal-to-noise ratio of these dichroic spectra is good considering

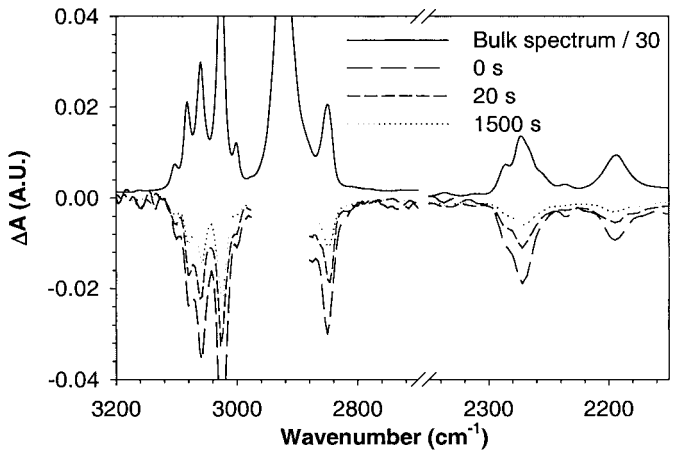

Figure 1. Infrared spectrum of an undeformed PS 942 / dPS 200 blend (bulk spectrum / 30), and dichroic difference spectra recorded at the end of the deformation (0 s), and after 20 and 1500 s of relaxation.

that the maximum ΔA is smaller than –0.02 for the C-D stretchings and that the acquisition time was 1.6 s for the 0 and 20 s spectra. The dichroic difference of all bands is negative, indicating that the transition moments associated with these vibrations are perpendicular to the deformation direction. In this work, the symmetric CH_2 stretch at 2850 cm^{-1} and the aromatic C-D stretch at 2273 cm^{-1} have been used to characterize the long PS and the short dPS chains, respectively. The antisymmetric CH_2 stretching band at 2920 cm^{-1} has been masked in the difference spectra because it was saturated.

It is obvious from the evolution of the dichroic differences in Figure 1 that both components of the blend relax toward the isotropic state as a function of time. In order to determine quantitatively the orientation function, $\langle P_2 \rangle$, the α angle of the bands must be known. We have shown in a previous paper that this angle is 90° for the 2850 cm^{-1} band.[16] To determine the α angle of the 2273 cm^{-1} band, a blend containing 75% of PS 200 and 25% of dPS 200 has been deformed at Tg + 8. In such a blend, the orientation of both PS and dPS should be identical since their molecular weight is very similar. Figure 2 shows that superimposable relaxation curves are obtained when an α angle of 80° is used for the C-D symmetric stretching, in general agreement with the value of 73° reported

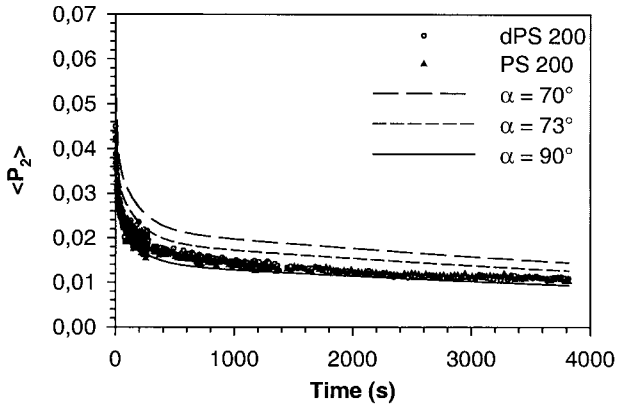

Figure 2. Relaxation curves for a PS 200 / dPS 200 blend following a deformation at Tg + 8. The curves represent the $<P_2>$ values calculated for dPS 200 using different α angles.

elsewhere.[9,13] The orientation functions that would have been obtained for dPS 200 using α angles of 70, 73 and 90° are also shown, allowing an estimate of the uncertainty on the angle. These angles yield $<P_2>$ values 40 and 22 % above and 10% below those obtained for PS 200, respectively. The discrepancy between the angle found in this study and in the previous ones can be explained by the use of different reference bands for the calculation of the orientation of the hydrogenated PS, namely the 2850 and 1028 cm^{-1} bands in this work and the 906 cm^{-1} band (assuming an α angle of 35°) in the previous studies.[9,13] We have already observed that different orientation functions are obtained for pure PS using these specific bands, although they possess rather well accepted α angles. This leads to believe that further work is still necessary in order to fully establish the absolute values of these α angles. It is interesting to note that the relaxation curve obtained using the 3061 cm^{-1} band is also superimposable with the curves of Figure 2 if the same α angle of 80° is used to calculate its orientation function. Since this band is assigned to an in-plane aromatic C-H stretch,[17] it is not surprising to observe a similar angle as that for the 2273 cm^{-1} band.

Figure 3 shows the evolution of the orientation function during deformation at Tg + 8 for pure PS 942 and for blends of PS 942 with dPS 20, 60, and 200. Although a certain scattering is present in the data, it appears that a single curve can acceptably describe the orientation of both long and short chains for all samples. This indicates that a strong orientational coupling exists between the short chains and the matrix during the deformation process. Although dPS 20 possesses a

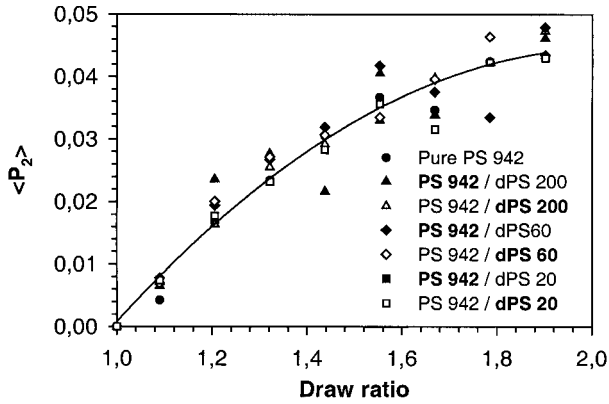

Figure 3. Evolution of the orientation function of PS and dPS in the various blends during deformations at Tg + 8. Filled and open symbols refer to PS and dPS, respectively. The curve is only a guide to the eye.

molecular weight below M_e (about 36 kg/mol for PS), it also orients to the same level as the other samples. In the Doi-Edwards model, it is suggested that the first (fastest) relaxation time, attributed to the Rouse relaxation of the segments between the entanglement junctions of the network, is molecular weight independent.[18] In previous studies, the first relaxation time of PS for deformations slightly above Tg has been estimated to be of the order of a few seconds.[16,19,20] In this context, it is less surprising to observe similar orientations for all samples since limited relaxation has time to occur during stretching to a draw ratio of 2 (12 s). This is in contrast to the results of Siesler et al., who observed a marked molecular weight dependence for the orientation of the short chains during deformation.[13] In that case, however, samples were stretched to a draw ratio of 4, thus allowing sufficient time (69 s) for molecular weight-dependent relaxation processes, such as the chain retraction, to occur during the last part of the deformation.

Figures 4 and 5 show the relaxation curves obtained directly by PM-IRLD for pure PS 942 and for the various blends following deformation at Tg + 15 at a drawing speed of 100 cm/min. Such a rapid deformation rate was used to ensure that no significant relaxation could occur during the short 1.3 s stretching. Even though Figure 3 shows that the deformation curves are similar, the relaxation process shows a large molecular weight effect for the short dPS chains as well as for the long PS chains composing the matrix. For all systems, the long chains present a higher orientation and slower relaxation dynamics than the short chains. In Figure 4, it can be observed that the addition of the low molecular weight dPS accelerates the relaxation rate of the matrix as compared

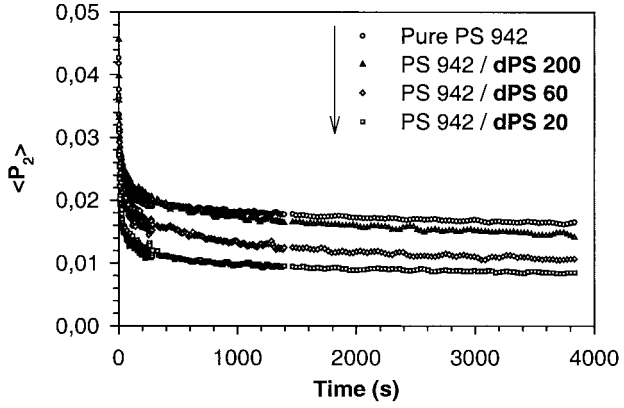

Figure 4. Relaxation curves of PS 942 in the different blends following a deformation at Tg + 15. The arrow indicates the order of the curves.

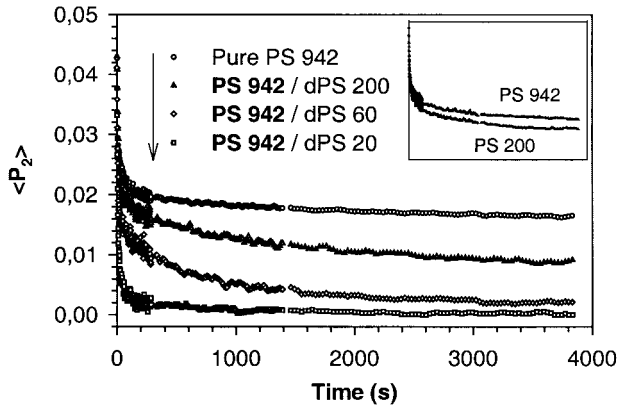

Figure 5. Relaxation curves of dPS of various molecular weights in blends with PS 942 following a deformation at Tg + 15. The arrow indicates the order of the curves. The inset shows the relaxation curves of dPS 200 in blends with PS 200 and PS 942 following a deformation at Tg + 8.

to that for the homopolymer. The influence of the short chains can be clearly observed for all dPS, in contrast to previous work in which such influence appeared to be restricted to chains shorter than M_c.[11,13] This effect can be explained by considering that the faster relaxation of the short chains releases topological constraints that maintain the long chains in their deformed tube.[14] The matrix chains in the blends can therefore retract at a faster rate as compared to those in pure PS 942. When dPS chains are shorter than M_c, they do not form entanglements with the matrix,

therefore reducing the network density of the long chains and further increasing their relaxation rate. The apparent absence of effect of blending on the orientation relaxation of the long chain in ref. 5 could be explained by a too short spawn of the relaxation curves, which were measured for 130 s. Indeed, the difference between the relaxation kinetics in pure PS 942 and in its blend with dPS 200 is only apparent after 700 s of relaxation in Figure 4, and would in consequence have been missed with a shorter experimental measurement time. It should be noted that a slight difference in the relaxation of the long chains in the pure PS 200 and in its blend with dPS 72 seems to appear in Figure 3 of ref. 5 after about 50 s of relaxation, in agreement with the previous suggestion.

The influence of the molecular weight of the short chains on their relaxation is shown in Figure 5. As expected from theoretical models,[18] the effect is gradual and is larger than that observed in Figure 4 for the blend matrix. While blending accelerates the relaxation of the long chains, it decreases the relaxation rate of the short deuterated PS as compared to that observed for the pure short homopolymer. As an example, the relaxation curves of dPS 200 in its blend with PS 200 (equivalent to a pure dPS 200) and with PS 942 after a deformation at Tg + 8 are shown in the inset of Figure 5. The accuracy of the PM-IRLD results as compared to conventional IRLD allows observing with confidence that the relaxation kinetics of dPS 200 is hindered in the PS 942 matrix as compared to that in the "pure" dPS 200. This phenomenon can be explained using a similar argument as before: the presence of the slowly relaxing oriented long chains induces more topological constraints on the deformed tube of the short species in the blend as compared to the homopolymer. This reduces the constraint release and results in a slower relaxation. It can be noted that the short time relaxation behavior is the same for dPS 200 in the two blends, in agreement with the fact that the Rouse relaxation between entanglement junctions is molecular weight independent.

Because of their weak or inexistent entanglement network, films of pure dPS 20 and dPS 60 can not be deformed to a draw ratio of 2 without breaking, thus preventing a direct comparison of their behavior in the pure state and in blends. Nevertheless, using the first relaxation time as determined by PM-IRLD for pure PS 942[16] and the scaling laws of the Doi-Edwards model,[18] relating the relaxation times to the molecular weight of the chains, it can be calculated that if they were stretched in the pure state, dPS of 20 and 60 should be fully relaxed in less than 25 and 540 s, respectively. Although the signal-to-noise ratio in the spectra does not allow making quantitative statement about the long-time orientation of dPS 20 ($<P_2>$ values below 0.001), Figure 5 shows that the orientation functions of the deuterated chains do not reach a value of zero even for

relatively long times. This residual orientation is in agreement with the observations of previous studies on bimodal polymer blends and can be explained by a nematic coupling of the short chains with its oriented surrounding.[10,21] This result constitutes a further confirmation of the importance of the orientation of the environment on the relaxation kinetics of a polymer chain.

Molecular orientation in single *Bombyx mori* silk fibroin fibers

Spider and silkworm silk filaments are among nature's most highly engineered structural materials, achieving, in some cases, combinations of strength and toughness that could not be reproduced by artificial means. The simple amino acids glycine, alanine, and serine, account for approximately 85% of the total amino acids of *B. mori* silk fibroin. Like other natural fibrous proteins, the primary structure of silk fibroin has a highly repetitive sequence with alternating (Gly-Ala-Gly-Ala-Gly-Ser)$_n$ domains separated by more complex regions containing amino acids with bulkier side chains. Because of its peculiar block copolymer structure, composed of hard and soft segments, it is now well accepted that *B. mori* silk fibroin is a semicrystalline biopolymer made of amorphous flexible chains reinforced by small stiff crystallites. The crystalline regions, which are arranged in antiparallel β-sheets, are responsible for the silk tensile strength. Characterization of the *B. mori* silk fibroin structure by Raman spectroscopy has been the subject of several studies,[22-25] but the degree of orientation has never been quantitatively determined before.

Figure 6 shows the Raman spectra between 600 and 1800 cm^{-1} of a degummed silk thread with

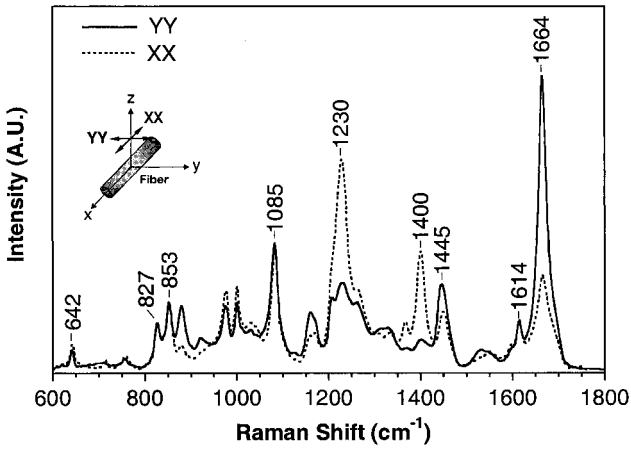

Figure 6. Polarized Raman spectra of a degummed cocoon fiber of *Bombyx mori*.

both the incident and scattered radiation polarized either parallel (XX) or perpendicular (YY) to the fiber axis. As can be seen, the use of state-of-the-art Raman instrumentation with a microscope allows the *in situ* recording of high quality spectra of single fibers possessing a diameter under 20 μm in a very short acquisition time. Spectra similar to those of Figure 6 were obtained by Shao et al.[23] using the 633.8 nm excitation and by rotating the fiber under the laser beam instead of the laser polarization. The spectra of Figure 6 are dominated by the strong bands due to the conformationally sensitive amide I and amide III vibrations that are located at 1664 and 1230 cm^{-1}, respectively. Both the shape and the position of these bands indicate clearly that *B. mori* silk fibroin has a high β-sheet content.[22,26-29] One can also notice that the intensity of the amide bands depends strongly on the polarization of the incident radiation. The amide I band is sharp and much more intense for the YY polarization while the major component of the amide III band is stronger when both the incident and scattered radiation are polarized parallel to the fiber axis. Since the carbonyl groups are perpendicular to the protein backbone while the C-N bonds are more parallel to the chain axis in the β-sheet structure, the relative intensity of the amide I and III bands qualitatively indicates that the β-sheets are orientated parallel to the fiber axis,[25] as illustrated in Scheme 1.

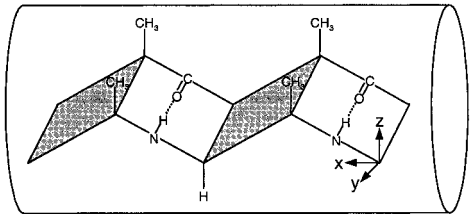

Scheme 1: Proposed model for the orientation of the β-sheets in a silk fiber.

In addition to the amide modes, several amino acid side chains also give rise to strong bands in the Raman spectra of silk. The band at 1400 cm^{-1} is associated to the symmetric stretching mode of the carboxylate groups found in ionized glutamic acid (Glu) and aspartic acid (Asp) residues. As seen in Figure 6, the carboxylate groups are also highly oriented along the fiber axis since the 1400 cm^{-1} band is much stronger in the XX polarized spectrum. According to the amino acid sequence previously determined by Mita et al.,[30] Glu and Asp residues, which are the only charged amino acids having the carboxylate group as a side chain, are present in small amount in *B. mori* silk and are thought to be located in the β-bends found between the antiparallel β-sheets.[31] The band at 1085 cm^{-1} is assigned to the C-C stretching mode of the protein backbone while the 1445 cm^{-1}

band is due to the bending mode of the methylene and methyl groups.[23,24] Methyl groups are particularly abundant in cocoon silk since the glycine content is estimated to 46% of the total amino acids.[31] It is well known that the symmetric vibrations of polarizable molecules, such as aromatic rings, give rise to very strong Raman lines. Even though *B. mori* cocoon fibers contain only 5% of tyrosine residues,[31] the well-defined bands that appear at 642, 827, 853, 1002 and 1614 cm^{-1} are due to aromatic side chain of the tyrosine residues.[32] Qualitatively, one can see from Figure 6 that the tyrosine residues are not oriented.

To obtain more quantitative information about the orientation of the *B. mori* silk fibroin, we have used the method proposed by Sourisseau and coworkers for systems that possess a uniaxial fiber symmetry. With this method, $\langle P_2 \rangle$ and $\langle P_4 \rangle$ are determined from the two following intensity ratios:

$$R_1 = \frac{I_{YX}}{I_{YY}} \quad \text{and} \quad R_1 = \frac{I_{XY}}{I_{XX}}$$

where the I_{IJ} terms are the intensities for a given band in the four polarized spectra that can be measured by back-scattering Raman microspectroscopy.[33,34] Due to the limited number of spectra available in Raman microscopy, this method, which also takes into account the high numerical aperture of the microscope objective used to collect the scattered light, is valid only for vibrations having a diagonal Raman tensor with $\alpha_1=\alpha_2<<\alpha_3$. The validity of this assumption can be verified from the depolarization ratio, ρ, measured for an isotropic sample using the following expression:

$$\rho = \frac{I_{YX}}{I_{YY}} = \frac{(1-a_1)^2}{(8a_1^2+4a_1+3)}$$

where $a_1 = \alpha_1/\alpha_3$.[35] For the amide I vibration, we have observed that the depolarization ratio measured using a regenerated *B. mori* film is 0.21, thus showing that α_3 is approximately 10 times larger than α_1.

Figure 7 shows the XX and YY polarized Raman spectra in the amide I region obtained for a fiber of *B. mori* silk fibroin and for a regenerated film. The broad shape of the amide I band observed for the film and the nearly equal intensity for the XX and YY spectra suggest that the chains are rather disordered in the regenerated film. Indeed, the calculated $\langle P_2 \rangle$ value for the amide I band is, within the experimental error, very close to zero ($\langle P_2 \rangle$ = -0.02 and $\langle P_4 \rangle$ = 0.22), indicating that the orientation of the polypeptide chains in the regenerated film is very low. This result shows that the calculation procedure used to determine the $\langle P_2 \rangle$ and $\langle P_4 \rangle$ coefficients is valid for the amide I vibration that is essentially associated with the C=O stretching vibration of the peptide group.[36]

In contrast, the large intensity difference between the XX and YY spectra of *B. mori* silk fibroin

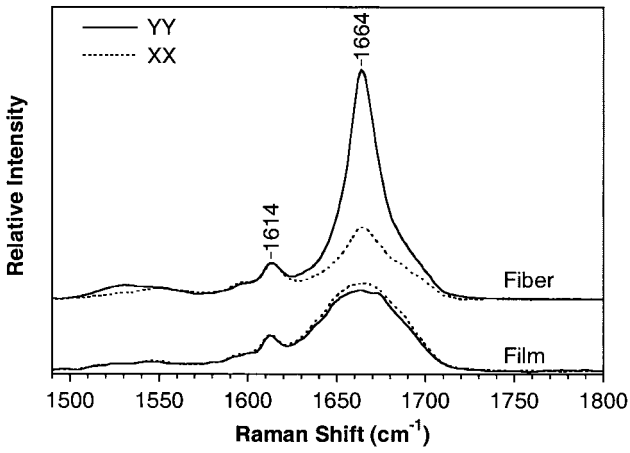

Figure 7. Polarized Raman spectra in the amide I region for a degummed cocoon fiber and a regenerated film.

indicates that the β-sheets are highly ordered in the cocoon fiber. For each fiber, spectra were recorded from three points equally spaced by 50 μm and a total of four fibers were analyzed. The results indicate that the β-sheets are homogenously distributed and oriented within a fiber but that slight variations in the level of orientation occurs between different fibers. The average $\langle P_2 \rangle$ and $\langle P_4 \rangle$ values calculated over the 12 measurements from the peak height intensity of the amide I band at 1664 cm^{-1} are -0.37 ± 0.07 and 0.29 ± 0.06, respectively. The $\langle P_2 \rangle$ value clearly shows that the peptide C=O groups are highly oriented perpendicular to the fiber axis, the maximum value of $\langle P_2 \rangle$ for perfect perpendicular orientation being -0.5. The majority of the β-sheets in *B. mori* silk fibroin are thus oriented parallel to the fiber axis. It has been shown that with the use of the information entropy theory, it is possible to obtain more accurate qualitative information about the shape of the orientation distribution if both the $\langle P_2 \rangle$ and $\langle P_4 \rangle$ coefficients are known.[37,38] Considering the $\langle P_2 \rangle$ and $\langle P_4 \rangle$ values given above, the distribution of orientation of the peptide C=O groups in these *B. mori* cocoon silk fibers should be bimodal with a major peak centered at 90° and a weaker one centered at 0° of the fiber axis.[38] The minor distribution of β-sheets that are oriented perpendicular to the fiber axis is most likely due to the folding of the antiparallel β-sheets that are parallel to the fiber axis. These preliminary results show that Raman microspectroscopy is a promising technique to quantitatively determine molecular orientation in silk monofilaments.

[1] I. M. Ward. "*Structure and Properties of Oriented Polymers*", Second ed.; Chapman & Hall: London 1997.
[2] T. Buffeteau; M. Pézolet. *Appl. Spectrosc.* **1996**, *50*, 948.
[3] T. Buffeteau; B. Desbat; M. Pézolet; J. M. Turlet. *J. Chim. Phys.* **1993**, *90*, 1467.
[4] M. Pigeon; R. E. Prud'homme; M. Pézolet. *Macromolecules* **1991**, *24*, 5687.
[5] T. Asakura; H. Kashiba; H. Yoshimizu. *Macromolecules* **1988**, *21*, 644.
[6] X. Chen; Z. Shao; N. S. Marinkovic; L. M. Miller; P. Zhou; M. R. Chance. *Biophys. Chem.* **2001**, *89*, 25.
[7] H. Yamada; H. Nakao; Y. Takasu; K. Tsubouchi. *Mat. Sci. Eng. C-Bio. S.* **2001**, *14*, 41.
[8] J. F. Tassin; L. Monnerie; L. J. Fetters. *Macromolecules* **1988**, *21*, 2404.
[9] J. F. Tassin; L. Monnerie; L. J. Fetters. *Polym. Bull.* **1986**, *15*, 165.
[10] J. F. Tassin; A. Baschwitz; J.-Y. Moise; L. Monnerie. *Macromolecules* **1990**, *23*, 1879.
[11] C. Hayes; L. Bokobza; F. Boue; E. Mendes; L. Monnerie. *Macromolecules* **1996**, *29*, 5036.
[12] L. Bokobza. *Macromol. Symp.* **1999**, *141*, 1.
[13] H. W. Siesler; C. Hayes; L. Bokobza; L. Monnerie. *Macromol. Rapid Commun.* **1994**, *15*, 467.
[14] S. Barsky; G. W. Slater. *Macromolecules* **1999**, *32*, 6348
[15] A. K. Kalkar; F. Pfeifer; H. W. Siesler. *Macromol. Chem. Phys.* **1998**, *199*, 667.
[16] C. Pellerin; R. E. Prud'homme; M. Pézolet. *Macromolecules* **2000**, *33*, 7009.
[17] S. Krimm. *Adv. Polym. Sci.* **1960**, *2*, 51.
[18] M. Doi. *J. Polym. Sci., Polym. Phys. Ed.* **1980**, *18*, 1005.
[19] J. F. Tassin; L. Monnerie. *Macromolecules* **1988**, *21*, 1846.
[20] L. Messé; M. Pézolet; R. E. Prud'homme. *Polymer* **2001**, *42*, 563.
[21] C. M. Ylitalo; J. A. Kornfield; G. G. Fuller; D. S. Pearson. *Macromolecules* **1991**, *24*, 749.
[22] P. Monti; G. Freedi; A. Bertoluzza; N. Kasai; M. Tsukada. *J. Raman Spectrosc.* **1998**, *29*, 297.
[23] Z. Shao; F. Vollrath; J. Sirichaisit; R. J. Young. *Polymer* **1999**, *40*, 2493.
[24] K. A. Trabbic; P. Yager. *Macromolecules* **1998**, *31*, 462.
[25] D. B. Gillepsie; C. Viney; P. Yager. In *Silk Polymers: Materials Science and Biotechnology*; A. S. Ser., Ed., 1994; Vol. 544, pp 155-167.
[26] P. R. Carey. "*Biological Applications of Raman and Resonance Raman Spectroscopies*"; Academic Press 1982.
[27] S. Krimm; J. Bandekar. In *Advances in Protein Chemistry*; I. Academic Press, Ed.: Toronto, 1986; Vol. 38, pp 181-364.
[28] S. Krimm. In *Biological Applications of Raman Spectroscopy*; T. G. Spiro, Ed.; Jonhn Wiley & Sons: New York, 1987; Vol. 1: Raman Spectra and the Conformations of Biological Macromolecules, pp 1-45.
[29] S. Zheng; G. Li; W. Yao; T. Yu. *Appl. Spectrosc.* **1989**, *43*, 1269.
[30] K. Mita. *J. Mol. Biol.* **1988**, *203*, 917.
[31] C. Z. Zhou; F. Confalonieri; N. Medina; Y. Zivanovic; C. Esnault; T. Yang; M. Jacquet; J. Janin; M. Duguet; R. Perasso; Z. G. Li. *Nucleic Acids Res.* **2000**, *28*, 2413.
[32] M. N. Siamwiza; R. C. Lord; M. C. Chen; T. Takamatsu; I. Harada; H. Matsuura; T. Shimanoxhi. *Biochemistry* **1975**, *14*, 4870.
[33] F. Lagugné Labarthet; T. Buffeteau; C. Sourisseau. *J. Phys. Chem. B* **1998**, *102*, 5754.
[34] F. Lagugné Labarthet; J.-L. Bruneel; T. Buffeteau; C. Sourisseau; M. R. Huber; S. J. Zilker; T. Bieringer. *Phys. Chem. Chem. Phys.* **2000**, *2*, 5154.
[35] F. Lagugné Labarthet; C. Sourisseau. *J. Raman Spectrosc.* **1996**, *27*, 491.
[36] T. Miyazawa; T. Shimanouchi; S.-I. Mizushima. *J. Chem. Phys.* **1958**, *29*, 611.
[37] H. Pottel; W. Herreman; B. W. van der Meer; M. Ameloot. *Chem. Phys.* **1986**, *102*, 37.
[38] F. Lagugné Labarthet; T. Buffeteau; C. Sourisseau. *Appl. Spectrosc.* **2000**, *54*, 699.